Creeping motion in granular flow

Benjamin A. Socie,[1] Paul Umbanhowar,[2,*] Richard M. Lueptow,[3] Nitin Jain,[1] and Julio M. Ottino[1,3]
[1]*Department of Chemical and Biological Engineering, Northwestern University, Evanston, Illinois 60208, USA*
[2]*Department of Physics and Astronomy, Northwestern University, Evanston, Illinois 60208, USA*
[3]*Department of Mechanical Engineering, Northwestern University, Evanston, Illinois 60208, USA*
(Received 7 October 2004; published 24 March 2005)

The core of a quasi-two-dimensional rotating cylinder filled more than half full with glass beads rotates slightly faster than the cylinder itself and decreases in radius over time. Core precession depends linearly on the number of tumbler revolutions while core erosion varies logarithmically. Both processes serve to quantify the slow granular motion in the "fixed" bed and depend on the filling fraction and the tumbler rotation rate. A simple model, based on experimental observations of an exponential decrease in velocity parallel to the free surface, captures the primary features of the core dynamics.

DOI: 10.1103/PhysRevE.71.031304 PACS number(s): 45.70.Mg, 45.70.Ht, 62.20.Hg, 83.10.Pp

Granular shear flows occur in many geologic [1] and industrial settings. Examples include snow, earth, and underwater avalanches, earthquake fault zones, grain beds adjacent to rapidly moving air or water, hoppers, chutes, and mixers. In the case of free surface flows, much attention has been focused on the regions of high shear. Only lately has it been realized, however, that there is also slow relative displacement of particles in what was traditionally considered "fixed bed" regions [2]. These slow relative motions are likely to significantly alter the stability, density, and mechanical response of the bulk material, enhance segregation and diffusion, and may be critical in cases where stability on geological time scales is important, such as in nuclear waste disposal. Therefore, a better understanding of shear induced creep flow will be of potential value in many areas spanning an array of disciplines.

Creeping flow in a fixed bed has been recently measured by Komatsu *et al.* in flow down a granular pile (heap) using long time scales to detect very slow velocities [2]. Below the flowing layer, a creep flow region was identified in which the velocity decreases exponentially with depth and with a characteristic length scale, y_0, on the order of a grain diameter, d. Velocity measurements indicating a similar creep flow region in quasi-two-dimensional rotating cylinders (tumblers) have also been reported [3,4].

Tumblers offer a convenient way to provide a constant driving force to a granular medium. Particles brought continuously to the surface by the rotation of the tumbler avalanche down the slope, are deposited, and then repeat the process. Motion occurs near the free surface in a lenslike region of maximum depth δ, which is typically 5–12 particles deep [4–8]. Particles in the flowing layer continually roll and slide about one another as they tumble down the free surface. A tumbler filled halfway or less with identical particles, except for color, becomes completely mixed within three or four tumbler revolutions because all particles pass through the flowing layer at least once per tumbler revolution.

For creep flow experiments, tumblers have the advantage that measurements can easily be made over long times. However, another important benefit comes from the ability to observe creep via the dynamics of the "invariant core"—a region at the center of the tumbler that does not pass through the flowing layer when the container is more than half-filled. Because the core never passes through the flowing layer, the conventional description of motion predicts that the core is in solid body rotation with the tumbler. That is, the initial conditions (unmixed particles) in the core will be preserved. For example, the interface between segregated materials, say white on the left and black on the right (Fig. 1), would move as if it were fixed to the container. This simple model is remarkably successful for predicting mixing. On much longer times scales, however, there is qualitative evidence that the core is dynamic. McCarthy *et al.* [9] reported that after about 40 tumbler revolutions, the core changes its angular position with respect to the tumbler, indicating that the core apparently rotates at a slightly different rate than the tumbler (core precession). Metcalfe *et al.* [10] observed the core to decrease in size over time (core erosion). Both papers, although preliminary in their investigations, note that core precession and erosion are strongly dependent on the particles used. Sugar balls, salt cubes, and sand particles all give very different precession and erosion rates under otherwise identical conditions.

Here we quantitatively examine the dependence of core erosion and core precession on the tumbler rotation frequency, ν, and the filling fraction, f, and we show how the core dynamics are driven by creeping motion beneath the flowing layer.

EXPERIMENT

A quasi-two-dimensional tumbler made of static dissipative acrylic, $R=8.88$ cm inner radius and $t=0.635$ cm (seven particles) thick, is driven at constant angular velocity by a computer-controlled stepper motor (see Fig. 2). The cell thickness is sufficient to prevent particles from becoming permanently jammed, but thin enough to suppress axial effects [11,12]. The cylindrical wall of the tumbler is covered

*Electronic address: umbanhowar@northwestern.edu

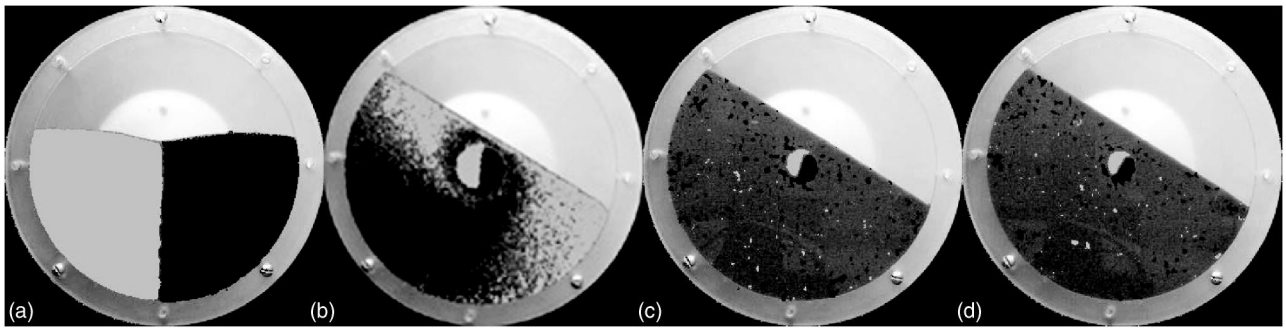

FIG. 1. Images of the tumbler after (a) 0, (b) 4, (c) 500, and (d) 1000 complete revolutions showing core development, precession, and erosion ($f=0.663$, $\nu=1$ rpm). The angular position of the tumbler is the same in all images, while the angular position of the core advances in the rotation direction (clockwise). A gray scale enhances contrast between the red (white) and blue (black) beads.

with 150-grit sandpaper to prevent particles from slipping. Spherical glass beads with diameter $d=0.89\pm0.05$ mm and colored with either red or blue Liquitex Glossies scratch-resistant acrylic enamel are used in all experiments. Initially, red beads are placed on one-half of the tumbler and an equal mass of blue beads is placed on the other, as shown in Fig. 1(a). The filling fraction, f, is defined as the ratio of the volume occupied by the particles, including the interstitial volume, to the total tumbler volume. For a core to form, the bottom of the flowing layer must lie above the cylinder's rotation axis, which requires f to be slightly greater than 0.5. An experiment consists of continuously rotating the tumbler for 1000 revolutions while taking images with a digital camera at a fixed orientation of the tumbler and at regular intervals—every revolution for the first 20 revolutions and every five revolutions thereafter. The tumbler rotation frequency is varied between 0.5 and 2.5 revolutions per minute (rpm). For $\nu<0.5$ rpm, discrete avalanches occur, while for $\nu\gtrsim2.5$ rpm, the free surface is no longer flat, but instead curves slightly upward on the lower side.

The core is defined as the essentially circular domain of unmixed particles at the center of the tumbler. It is identified by applying a spatial low pass filter with a cutoff length of approximately $4d$ to each color image. The combined area of the resulting uniform red and blue regions of unmixed particles is measured and the core radius is obtained as $r_c=\sqrt{(\text{area})/\pi}$. The orientation of the core is determined by the boundary between the red and blue particles. Since the boundary is typically curved at the outer radius of the core, only the center 75% of the core is used to determine the orientation. An ellipse is fit to the pixels along the boundary, and the core orientation is determined by the direction of the major axis of the ellipse.

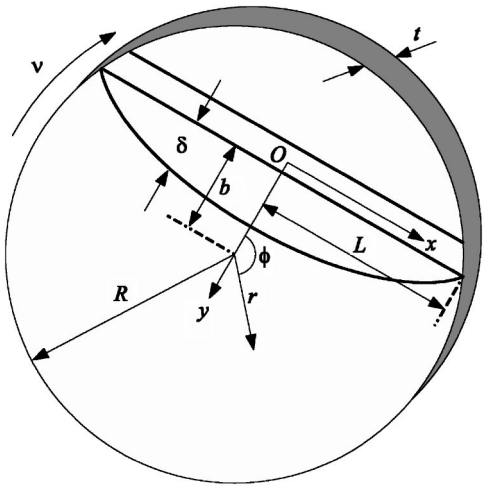

FIG. 2. The rotating tumbler geometry with the coordinate systems and the system parameters.

CORE DYNAMICS

Images of a typical experiment after 0, 4, 500, and 1000 complete revolutions are shown in Fig. 1. The core becomes well-defined after approximately four tumbler revolutions [see Fig. 1(b)]. As rotation continues, the angle of the boundary between the two colors of particles in the core advances relative to the tumbler, as shown in Figs. 1(c) and 1(d). This is core precession. The difference between the core angle and its initial value is called the precession angle, θ. The change in θ per tumbler rotation is defined as the dimensionless precession rate, $m=\Delta\theta/2\pi=\dot{\theta}/(2\pi\nu)$. In addition to illustrating core precession, Fig. 1 shows that the core radius is smaller after 1000 revolutions than when formed; this is core erosion.

Figure 3(a) illustrates the increase of θ with the number of tumbler rotations, N, for several filling fractions. In each case, θ increases approximately linearly with N indicating that the precession rate is constant during each experiment. Furthermore, m is largest for the smallest filling fraction and goes nearly to zero for the highest filling fraction, as Fig. 3(b) shows. Figure 3 also shows that the precession rate is highly sensitive to small changes in filling fraction at low f and is relatively insensitive at high f. Based on Fig. 3(b), a practical filling fraction to assess the impact of the tumbler rotation rate is $f\sim0.7$. At this filling fraction, the precession rate is relatively insensitive to small variations in f, but it is still large enough to be measurable over time scales on which the experimental parameters are stable. Experiments are run consecutively, in order of alternately increasing and decreasing ν, so that the particles are all from the same batch of dye and the sandpaper in the tumbler is not significantly worn. Even with these precautions, there is some minor variation in

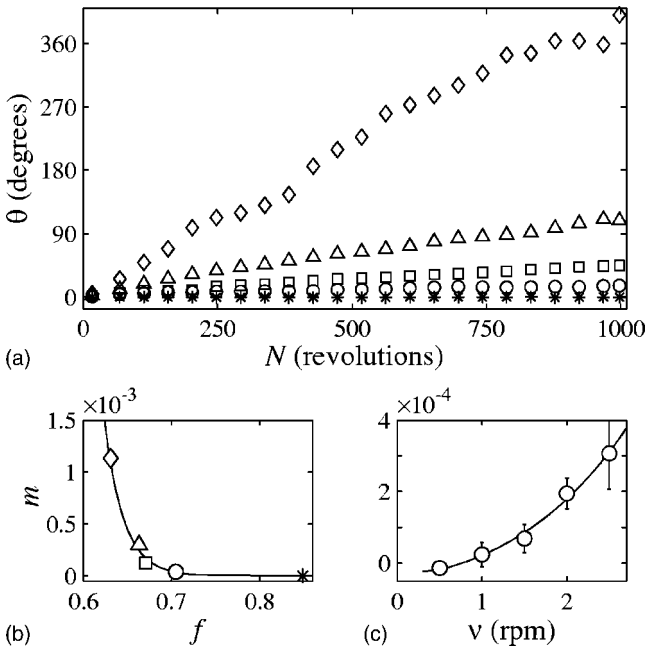

FIG. 3. (a) Evolution of the precession angle, θ, for different fill fractions: ◇, $f=0.631$; △, $f=0.663$; □, $f=0.671$; ○, $f=0.705$; *, $f=0.849$ ($\nu=1$ rpm). Data were taken every fifth revolution; values averaged over 45 rotations are shown. (b) The precession rate m vs f from (a); the solid curve is a fit to our model, which gives $y_0/d=3.4$. (c) Dependence of m on the tumbler rotation rate at $f=0.70$. The solid curve is a fit to our model, which also yields $y_0/d=3.4$, and according to which the primary mechanism for the increase in m with ν is the increase in the depth of the flowing layer δ. The uncertainty in f is ±0.003 in all cases.

the measured value of the precession rate. We speculate that this variation occurs because the filling fraction does not uniquely determine the state of the system: humidity, preparation history, details of the particle size distribution, and other factors are all expected to influence the results to some degree. Figure 3(c) shows m averaged over five experiments as a function of ν for $f=0.7$. The precession rate increases with ν. At the lowest rotation rate, $\nu=0.5$ rpm, m is small and slightly negative. We believe that this is due to slipping of the entire bed opposite to the rotation direction, since in preliminary experiments without sandpaper on the cylinder wall, this effect was significantly more pronounced.

The core radius decreases logarithmically with N for all filling fractions and with nearly equal slopes, as Fig. 4(a) shows, except at the highest values of f. Here, for $f=0.849$ and to a lesser extent for $f=0.705$, the core radius initially decreases logarithmically, but is nearly constant between 100 and 1000 revolutions. There is no systematic variation in the slope with f, and the initial core size, r_0, increases approximately linearly with f. In Fig. 4(b), r_c again decreases linearly with $\ln N$ for all ν, and the slope exhibits no systematic dependence on ν. At higher rotation frequencies, the initial core radius is slightly smaller than at smaller rotation frequencies.

VELOCITY PROFILE

It is clear from our experimental results that what has traditionally been called the fixed bed is, in fact, not fixed. Even particles that never enter the classically defined flowing layer move relative to one another, resulting in core erosion, and move relative to the tumbler, evident as core precession. The primary features of core precession and core erosion follow from a simple two-region model of the velocity field. To illustrate these different regions, Fig. 5 presents measurements of the particle velocity parallel to the flowing layer, u, acquired in the middle of the free surface and in a reference frame rotating with the tumbler. The data were obtained using the combined particle-image velocimetry (PIV) and particle-tracking velocimetry (PTV) measurement technique described in Ref. [4]. The decrease of velocity with depth in the flowing layer for our experiment is approximately linear and is described by $u_f=u_{max}-\dot{\gamma}y$, where y is the depth, u_{max} is the velocity at the surface, and $\dot{\gamma}$ is the shear rate. The exact functional form of the velocity profile in the flowing layer, which depends on the angle between the free surface and the angle of repose [13], does not affect the conclusions of our model. For depths greater than the flowing layer thick-

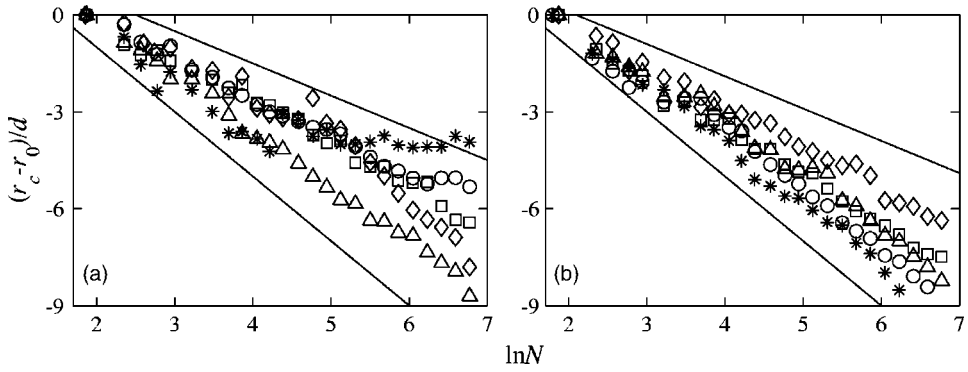

FIG. 4. (a) Decrease in scaled core radius, $(r_c-r_0)/d$ vs $\ln N$ for various filling fractions ($\nu=1$ rpm): ◇, $f=0.631$; △, $f=0.663$; □, $f=0.671$; ○, $f=0.705$; and *, $f=0.849$. (b) Dependence of $(r_c-r_0)/d$ vs $\ln N$ on ν for various rotation rates ($f=0.700$): ◇, $\nu=0.5$ rpm; △, $\nu=1$ rpm; □, $\nu=1.5$ rpm; ○, $\nu=2$ rpm; and *, $\nu=2.5$ rpm. In both (a) and (b) the slope of the data is nearly constant and matches the predictions of our model [Eq. (2)]. The slopes of the solid lines are -1 and -2 and correspond to characteristic length scales from our model of d and $2d$, respectively. Data were taken every fifth revolution; values averaged over fixed ratio intervals (1:1.2) are shown.

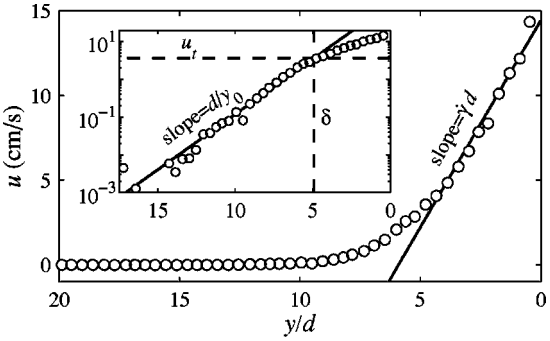

FIG. 5. Velocity parallel to the free surface vs scaled depth at the middle of the free surface measured using PIV/PTV velocimetry ($f=0.67$, $\nu=1$ rpm). The slope of the solid line gives $\dot{\gamma}=27.5\ \mathrm{s}^{-1}$. The inset, with a logarithmic ordinate, shows the exponential velocity regime; the solid line is a fit to $u_0 e^{-y/y_0}$ with $y_0=1.48d$ and $u_0=101$ cm/s, so $u_t=\dot{\gamma}y_0=3.62$ cm/s and $\delta=y_0\ln(u_0/u_t)=4.93d$. Data are analyzed in the reference frame of the rotating cylinder.

ness, δ, the rate of velocity decrease with increasing depth becomes exponential (inset of Fig. 5). Here the velocity is given by $u_e=u_0e^{-y/y_0}$, and is in accord with the results in Refs. [2–4] showing creeping motion below the flowing layer. Equating u_f and u_e with the characteristic velocity of the transition between the two regimes, u_t, gives the transition depth between the two regions, $\delta=(u_{max}-u_t)/\dot{\gamma}$, as well as $u_0=u_te^{\delta/y_0}$. Matching the shear rates at $y=\delta$ gives $u_t=\dot{\gamma}y_0$, which connects the characteristic physical quantities of the freely flowing and creeping flow regimes.

PRECESSION

Core precession can be modeled by considering the contribution of the velocity in the creep regime to the local angular velocity. The creep velocity is assumed to be parallel to the free surface, and its contribution to the radial velocity is ignored since the core remains virtually circular in the experiments. At a radial distance r from the rotation axis and at an angle ϕ away from perpendicular to the free surface, u_e produces an angular velocity $\dot{\theta}(r,\phi)=(u_0/r)e^{(r\cos\phi-b)/y_0}\cos\phi$ (see Fig. 2). Substituting in the expressions for u_0 and u_t and expanding the exponential near the center of the core ($r\ll y_0$), followed by averaging over ϕ and dividing by the rotation frequency of the tumbler, yields

$$m=\frac{\dot{\gamma}}{4\pi\nu}e^{(\delta-b)/y_0}. \tag{1}$$

Equation (1) has the following implications for core precession: (i) At constant ν and for $f<0.9$, the argument of the exponential is dominated by changes in $b\approx(\pi R/2)(f-1/2)$, so $m(f)\approx(\dot{\gamma}/4\pi\nu)e^{\delta/y_0}e^{-\pi R(f-1/2)/2y_0}$. The solid curve in Fig. 3(b) is a fit to this equation, which shows the exponential dependence of m on f, and which gives $y_0\approx3.4d$. (ii) At constant f and at the middle of the free surface, $\delta=L\sqrt{2\pi\nu/\dot{\gamma}}$, where L is one-half the free surface length [5]. Substituting this expression into Eq. (1) gives $m=(\dot{\gamma}/4\pi\nu)e^{-b/y_0}e^{(L/y_0)\sqrt{2\pi\nu/\dot{\gamma}}}$. The model predicts that at large ν, m will increase nearly exponentially with $\sqrt{\nu}$ [14]. The solid curve in Fig. 3(c) is a fit to this equation, which again gives $y_0\approx3.4d$. (iii) The primary assumption of our model is that u is independent of ϕ at constant depth. This assumption breaks down when the core is large because δ is no longer approximately constant and independent of ϕ due to the lens-like profile of the flowing layer. A second reason for the breakdown of this assumption is that the core radius can become larger than the free surface length. Both effects will lead to overestimates of m at large f. Additionally, the velocity field is not exactly parallel to the free surface far from the middle of the flowing layer, which also leads to overestimates of m.

EROSION

To model core erosion, we again consider the flow in the exponential velocity region and construct a diffusion coefficient D as the product of the particle diameter and the relative velocity difference across a particle, $d|du/dy|$. After simplifying, $D(r,\phi)=d^2\dot{\gamma}e^{(\delta-b)/y_0}e^{r\cos\phi/y_0}$. The variance of the particle position is $\sigma^2=Dt$ so that the total variance for a point rotating with the tumbler after N rotations is $\sigma^2=\int_0^{N/\nu}Ddt=(N/\pi\nu)\int_0^{\pi}Dd\phi=(Nd^2\dot{\gamma}/\pi\nu)e^{(\delta-b)/y_0}\int_0^{\pi}e^{(r\cos\phi)/y_0}\times d\phi$. The integral term is π times the modified Bessel function I_0, which, for $r\gg y_0$, has the limiting form $e^{r/y_0}/\sqrt{2\pi r/y_0}$. This expression is dominated by the exponential in our experiments so we take $I_0\sim Ce^{r/y_0}$, where C is a constant. With the assumption that the core becomes mixed when σ is $O(d)$, we set $\sigma=d$ and solve for the radius of the interface between mixed and unmixed regions (i.e., the core radius),

$$r_c(N)=(b-\delta)-y_0\ln\left(\frac{C\dot{\gamma}}{\nu}N\right)\equiv r_0-y_0\ln N. \tag{2}$$

Equation (2) predicts that r_c versus $\ln N$ should be linear with a slope equal to y_0, and that this slope should be independent of ν and f. To verify this prediction, Fig. 4 plots $(r_c-r_0)/d$ versus $\ln N$ and indicates that the slope is basically constant and corresponds to $-2<y_0/d<-1$ (solid lines in figure have slope -1 and -2). For the two largest f ($f=0.705$ and 0.849) in Fig. 4(a), the slope of r_c versus $\ln N$ is not constant over the entire range of N, but appears to saturate after $N\approx300$ and $N\approx100$ rotations, respectively. As was the case with the precession analysis and for the same reasons, the model predictions for core erosion are expected to be inaccurate for large cores and will lead to overestimates of the slope of r_c versus $\ln N$. Finally, the observed decrease in the initial core radius with increasing ν is explained by the increase in δ with increasing ν, as is discussed above for the case of precession.

DISCUSSION

Core precession and core erosion give information about the creeping motion below the freely flowing layer. Our model—based on an exponential velocity profile below the freely flowing layer—is in agreement with the results of core precession measurements, showing a linear dependence of

precession angle on N, an exponential decrease in the precession rate with increasing f, and a nearly exponential increase in m with increasing $\sqrt{\nu}$. The logarithmic dynamics of core erosion agrees well with our model except at the highest f where the model is expected to be inaccurate.

Two discrepancies between the model predictions and the experimental data should be noted. First, y_0 obtained from the precession measurements ($\approx 3.4d$) is larger than the value of $y_0 \approx 1.5d$ measured directly (Fig. 5) and obtained from the slope of r_c versus $\ln N$ (Fig. 4), and from the values in the literature of $1.4d$ and $2.5d$ from Refs. [2,3], respectively. In the latter case, there could be many reasons for this distinction, chief among these being differences in material properties and environmental factors. However, in the former case, the value of $3.4d$ obtained near the core for two independent data sets and the value of $1.5d$ obtained further from the core by way of PIV/PTV and the core erosion rate point to the possibility of a change in the functional form of the velocity profile between these two regions. Second, the constant precession rate obtained near the core center [Eq. (1)] should only be valid for $r \lesssim y_0$. At larger r, the local precession rate should increase and lead to a curved interface between the colored particles. A curved interface is visible in Fig. 1 near the outer core, but in the core interior, the interface is straight for $r > y_0$ in even the longest runs.

These inconsistencies suggest the possibility that the exponential decrease of velocity with depth is only valid over a finite depth interval. Our direct velocity measurements, as well as those of Komatsu *et al.* and Bonamy *et al.* [2,3], extend only to depths of 8–$12d$. For $f = 0.631$, our shallowest core, the core center is already about $17d$ below the freely flowing layer. Core erosion data would not be significantly affected by a modification in u_e until the depth of the top of the core was below the conjectural lower bound of the exponential scaling region. A modification of the exponential profile could be universal or may instead be unique to tumblers. In a tumbler, after a group of particles pass through the flowing layer they come to rest in a locally stable orientation. However, the forces exerted by gravity, other particles, and the container walls change as the tumbler turns. Eventually the local configuration may become unstable causing a rearrangement. If it occurs before the group has rotated by $\pi/2$, the core will advance; if it happens after $\pi/2$, the core will recede.

It is also important to remark that, as noted, the presence of walls affects the velocity field and other global properties such as the angle of repose in the tumbler as well as in other laterally confined free surface granular flows [15]. Possibly, the onset of the creep flow regime is related to the transfer of weight to the walls via frictional forces and is related to the Janssen effect [16] in which the pressure in a column of grains saturates at depths comparable to the width of the container. However, in terms of the model presented here, the wall interactions are expected to influence the values of constants (e.g., $\dot{\gamma}$ and δ), but not the functional form of u_e.

Erosion and precession in a tumbler are observable consequences of slow creeping motions in granular beds. Measurements of these processes lead to modifications of the conventional understanding of granular flow in a quasi-two-dimensional rotating tumbler. More importantly, however, is the possibility that quasi-two-dimensional tumblers can be used as diagnostic tools to investigate the creep flow of materials. Important questions remain: how do particle characteristics, e.g., roughness and shape, affect the creeping flow, what is the influence of the finite thickness of the container, and what, if any, modifications must be made to the exponential velocity profile far below the freely flowing layer in tumbler driven and other free surface granular flows.

ACKNOWLEDGMENTS

This work was supported by the Engineering Research Program of the Office of Basic Energy Sciences of the Department of Energy.

[1] *Particulate Gravity Currents*, Special Publication of the IAS, No. 31, edited by W. McCaffrey, B. Kneller, and J. Peakall (Blackwell Science, Malden, MA, 2001).
[2] T. S. Komatsu, S. Inagaki, N. Nakagawa, and S. Nasuno, Phys. Rev. Lett. **86**, 1757 (2001).
[3] D. Bonamy, F. Daviaud, and L. Laurent, Phys. Fluids **14**, 1666 (2002).
[4] N. Jain, J. M. Ottino, and R. M. Lueptow, Phys. Fluids **14**, 572 (2002).
[5] D. V. Khakhar, A. V. Orpe, and J. M. Ottino, Adv. Complex Syst. **4**, 407 (2001).
[6] N. Jain, J. M. Ottino, and R. M. Lueptow, J. Fluid Mech. **508**, 23 (2004).
[7] A. V. Orpe and D. V. Khakhar, Phys. Rev. Lett. **93**, 068001 (2004).
[8] K. M. Hill, G. Gioia, and V. V. Tota, Phys. Rev. Lett. **91**, 064302 (2003).
[9] J. J. McCarthy, T. Shinbrot, G. Metcalfe, J. E. Wolf, and J. M. Ottino, AIChE J. **42**, 3351 (1996).
[10] G. Metcalfe, L. Graham, J. Zhou, and K. Liffman, Chaos **9**, 581 (1999).
[11] J. Duran, *Sands, Powders, and Grains* (Springer, New York, 2000).
[12] G. H. Ristow, *Pattern Formation in Granular Materials* (Springer-Verlag, Berlin, 2000).
[13] L. E. Silbert, J. W. Landry, and G. S. Grest, Phys. Fluids **15**, 1 (2003).
[14] The predictions of our model are only valid in the continuous flow regime. For small ν, discrete avalanches occur, while for large ν, cataracting and centrifuging is observed.
[15] See, for example, S. Courrech du Pont, P. Gondret, B. Perrin, and M. Rabaud, Europhys. Lett. **61**, 492 (2003); N. Taberlet, P. Richard, A. Valance, W. Losert, J. M. Pasini, J. T. Jenkins, and R. Delannay, Phys. Rev. Lett. **91**, 264301 (2003), and references therein.
[16] H. A. Janssen, Z. Ver. Dtsch. Ing. **39**, 1045 (1895).